ISSN: 2277-3754
International Journal of Engineering and Innovative Technology (IJEIT)
Volume 1, Issue 4, April 2012

Mutualism Particle Swarm Optimization with TSK-type Fuzzy Controllers for Constructing a Laryngeal Image-based on LRAGD Diagnosis System

Cheng-Hung Chen, Hsien-Tse Chen, Sheng-Fuu Lin

Abstract—***This paper proposes TSK-type fuzzy controllers (TFC) with a mutualism particle swarm optimization (MPSO) for constructing a laryngeal image-based laryngopharyngeal reflux associated gastrointestinal diseases diagnosis system (LRAGD-DS). The proposed MPSO is based on cooperative evolution which each particle in the swarm represents only partial solution. The whole solution consists of several particles. The MPSO is different from the traditional cooperative evolution; with each swarm in the MPSO is divided into several groups. Each group represents a set of the particles that belong to only one fuzzy rule. Moreover, in the MPSO, each particle represents a single fuzzy rule and each particle in each swarm evolves separately. In the LRAGD-DS, the TFC-MPSO is used to train the LRAGD-DS. After training by the TFC-MPSO, the LRAGD-DS can diagnose the situation of LRAGD from laryngeal video clips automatically. The performance of the MPSO achieves excellently compared with other existing fuzzy models in the LRAGD-DS.***

Index Terms—**TSK-Type Fuzzy Controllers; Particle Swarm Optimization; Laryngopharyngeal Reflux.**

I. INTRODUCTION

In recent years, the concept of the fuzzy logic or artificial neural networks for control problems has grown into a popular research area [1]-[3]. The reason is that classical control theory usually requires a mathematical model for designing controllers. The inaccuracy of mathematical modeling of plants usually degrades the performance of the controllers, especially for nonlinear and complex control problems [4]-[5]. Fuzzy logic has the ability to express the ambiguity of human thinking and translate expert knowledge into computable numerical data.

A fuzzy system consists of a set of fuzzy IF-THEN rules that describe the input-output mapping relationship of the networks. Obviously, it is difficult for human experts to examine all the input-output data from a complex system to find proper rules for a fuzzy system. To cope with this difficulty, several approaches that are used to generate the fuzzy IF-THEN rules from numerical data have been proposed [1], [2], and [3]. In the design of a fuzzy controller, adjusting the required parameters is important. To do this, back-propagation (BP) training was widely used in [1], [2]. It is a powerful training technique that can be applied to networks with a forward structure. Since the steepest descent technique is used in BP training to minimize the error function, the algorithms may reach the local minima very fast and never find the global solution. For solving these problems, recently, several evolutionary algorithms, such as genetic algorithm (GA) [6], genetic programming [7], evolutionary programming [8], and evolution strategies [9], have been proposed. They are parallel and global search techniques. Because they simultaneously evaluate many points in the search space, they are more likely to converge toward the global solution. For this reason, an evolutionary method using for training the fuzzy model has become an important field.

The evolutionary fuzzy model generates a fuzzy system automatically by incorporating evolutionary learning procedures [10]-[17], where the well-known procedure is the genetic algorithms (GAs). Several genetic fuzzy models, that is, fuzzy models augment by a learning process based on GAs, have been proposed [10]-[13]. In [10], Karr applied GAs to the design of the membership functions of a fuzzy controller, with the fuzzy rule set assigned in advance. Since the membership functions and rule sets are co-dependent, simultaneous design of these two approaches will be a more appropriate methodology. A GA-based fuzzy controller [11] design method is proposed for a two-wheeled mobile robot to independently control two velocities of its left-wheeled motor and right-wheeled motor so that the controlled robot can move fast and efficiently to the desired position. A PSO-based method [12] is proposed to automatically determine appropriate membership functions of these two fuzzy systems so that the controlled robot can move to any desired position effectively in a two-dimensional space. In [13], Juang et al. proposed genetic reinforcement learning in the design of fuzzy controllers. The GA adopted in [13] was based upon traditional symbiotic evolution which, when applied to fuzzy controller design, complemented the local mapping property of a fuzzy rule. In [14], Tang proposed a hierarchical genetic algorithm. The hierarchical genetic algorithm enables the optimization of the fuzzy system design for a particular application. Juang [15] proposed the Combination of online clustering and Q-value based GA for reinforcement fuzzy system (CQGAF) to simultaneously design the number of fuzzy rules and free parameters in a fuzzy system. Lin [16] proposed a sequential-search based dynamic evolution (SSDE) to let better particles will be initially generated while better mutation points will be determined for performing dynamic-mutation. In [17], Lin proposed a hybrid evolution learning algorithm (HELA). The HELA combines the compact genetic algorithm (CGA) and the modified variable-length genetic algorithm, performs the structure/parameter learning for constructing the network dynamically. However, these approaches encounter one or more of the following major problems: 1) all the fuzzy rules are encoded into one chromosome; 2) the population cannot evaluate each fuzzy rule locally.

Recently, several researches have been applied neural fuzzy network to medical diagnosis system [18]-[25]. Genetic algorithm optimized fuzzy neural network (GA-FNN) proposed by Levente *et al.* [18] is capable of greatly assisting medicinal chemists in the design of lead compounds for HIV-1 protease, as well as for other therapeutically important enzymes. Benamrane et al. [19] propose an approach for detection and specification of anomalies present in medical images. The idea is to combine three metaphors: Neural Networks, Fuzzy Logic and Genetic Algorithms in a hybrid system. The advanced fuzzy cellular neural network (AFCNN) Wang et al. [20] proposed the advanced fuzzy cellular neural network (AFCNN), as a variant of the fuzzy cellular neural network (FCNN), is proposed to effectively segment CT liver images. The improved fuzzy cellular neural network (IFCNN) proposed by Wang et al. [21] has the global stability and the experimental results for microscopic white blood cell to demonstrate its obvious advantage over FCNN in keeping the boundary integrity. Subasi [22] proposed a dynamic fuzzy neural network (DFNN) that detection of epileptic seizure allows for the incorporation of both heuristics and deep knowledge to exploit the best characteristics of each. Neural network-based fuzzy model proposed by Lin et al. [23] can automatically identify a set of appropriate fuzzy inference rules and refine the membership functions through the steepest gradient descent learning algorithm. Chowdhury and Saha [24] proposed a fuzzy neural network used for the initial diagnosis of patients through an FPGA based on implementation of a smart instrument. Ebadian *et al.* [25] proposed fuzzy clustering and artificial neural network to predict coronary artery disease (CAD) in acute phase from planar and gated SPECT nuclear medicine images.

In this paper, as same with [18]-[25], we also proposed neural fuzzy network to constructing a diagnosis system. Therefore, TSK-type neural fuzzy network (TFC) with a mutualism particle swarm optimization (MPSO) is proposed for constructing a laryngeal image-based laryngo pharyngeal reflux associated gastrointestinal diseases diagnosis system. In laryngopharyngeal reflux, the reflux ate is that portion of gastrointestinal content backflows upwards through the esophagus to the larynx and pharynx. Various degrees of burns and inflammations are caused by gastrointestinal content in this manner. A number of diseases in the gastrointestinal tract may co-exist with laryngopharyngeal reflux, including gastritis, duodenitis, reflux esophagitis (RE), gastric ulcer (GU), and duodenal ulcer (DU), which are defined as laryngopharyngeal reflux associated gastrointestinal diseases (LRAGD) in this paper. To establish the diagnosis of LRAGD needed upper gastrointestinal pan ends copy (UGI-PES) examination, which much more suffers patients than the flexible laryngoscope examination. However, the treatment of LRAGD is different; depend on the severity of mucosa injury in the gastrointestinal tract: gastritis or duodenitis needed only antacid, RE, GU and DU need proton pump inhibitors. Moreover, the patients of laryngopharyngeal reflux did not totally suffered from LRAGD, some patients may still normal gastrointestinal mucosa. If we can diagnose the LRAGD from the laryngeal image which capture from the video clip of the flexible laryngoscopy examination automatically by a computer-assistant diagnosis system, we can arrange UGI-PES for candidate patients more precisely and save lots of negative screening procedure, also save some patients from the sufferance of examination then save the medical cost of examination.

Physicians often examine the degree of damage to laryngopharyngeal segment through flexible laryngoscopy to diagnose the laryngopharyngeal reflux. A scoring system of signs called reflux finding score (RFS) had been proposed by Belafsky et al. [26] in 2001. However, the score may be biased by physicians' personal subjective factors, and there are still some controversies on how to decide the weighted percentage for every item, so it was not widely used as standard. Some different suggestions were addressed in the studies conducted by Hill et al. [27] and Beaver et al. [28]. For RE, the damage level of esophageal mucosa can be seen directly through endoscopy. In 2000, Arango et al. [29] suggested using the level of esophageal mucosal break as the basis, and evaluating the severity of reflux esophagitis based on the Los Angeles (LA)classification (grades A – D, slight to severe). Currently, there is no diagnosis system available to make the correlation of laryngeal image findings with LRAGD.

For the literature of laryngeal images analyzed via a computer, Hanson et al. [30] sampled artificially in the bilateral vocal cords and interarytenoid area using 5x5 pixel blocks in 1998, which were then analyzed with Photoshop software using the red index = red / (red + green + blue). Analyzing the laryngeal images of seven normal volunteers and 64 patients, they found that there were some differences. After treatment, the red index in patients' images decreased. However, artificial sampling is time-consuming, so it is not beneficial for clinical diagnosis. In 2003, a paper which was conducted by Ilgner et al. [31] using artificial sampling and texture analysis. They focused on the vocal cords in studying laryngitis. Digital images were used by Beaver et al. [28] in 2003, but their results were still artificial interpretation. Furthermore, Men et al. [32] used laryngeal computerized tomography (CT) to scanning images for the reconstruction of laryngeal 3D images in 2007. Their purpose was to

ISSN: 2277-3754
International Journal of Engineering and Innovative Technology (IJEIT)
Volume 1, Issue 4, April 2012

diagnose diseases such as laryngo-carcinoma and tumor. For constructing a computer-assistant diagnosis system of laryngeal image, there is no automatic system currently available for the image capture, segmentation and feature extraction.

In this paper, we used laryngeal image sequences captured by the flexible laryngoscopy as the input value. The system looks for appropriate images and segments the characteristic zones in laryngeal images automatically, such as the vocal cords and posterior larynx. A large number of laryngeal video clips from patients of laryngopharyngeal reflux were collected for analysis and comparison according to the severity of the LRAGD. We hope to use laryngoscopic image as the basis of diagnosis to find differences in characteristics between various kinds of LRAGD, in order to suggest laryngologist to decide whether the patient should only receive medication or needs further UGI-PES examination. The advantage of the LRAGD-DS is that the situation of LRAGD can be diagnosis automatically from the video clips of flexible laryngoscopy examination.

In this paper, TSK-type fuzzy controllers (TFC) are used to construct a LRAGD-DS. Therefore, a TFC can diagnosis the situation of LRAGD automatically. For training the TFC robust, in this paper, a mutualism particle swarm optimization (MPSO) is proposed. In the proposed MPSO, each particle represents only one fuzzy rule; selecting and combining *n* particles from several groups construct an *n*-rules fuzzy system. The MPSO promotes both cooperation and specialization, which ensures diversity and prevents a swarm from converging to suboptimal solutions. Compare with the normal cooperative evolution, there are several groups in the swarm in the proposed MPSO method. Each group represents a set of the particles that belong to a fuzzy rule. For letting the groups that perform well can be corporate to generate better generation. The advantages of the proposed MPSO are summarized as follows: 1) The MPSO uses group-based swarm to evaluate the fuzzy rule locally. 2) It indeed can obtain better performs and converge more quickly than some traditional genetic methods.

II. STRUCTURE OF TSK-TYPE FUZZY CONTROLLERS

A Takagi-Sugeno-Kang (TSK) type fuzzy controller (TFC) [33] employs different implication and aggregation methods than the standard Mamdani controller. Instead of using fuzzy sets the conclusion part of a rule, is a linear combination of the crisp inputs.

IF x_1 is A_{1j} (m_{1j}, σ_{1j}) and x_2 is A_{2j}(m_{2j}, σ_{2j})…and x_n is A_{nj} (m_{nj}, σ_{nj})

THEN $y'=w_{0j}+w_{1j}x_1+\ldots+w_{nj}x_n$ (1)

Since the consequence of a rule is crisp, the defuzzification step becomes obsolete in the TSK inference scheme. Instead, the control output is computed as the weighted average of the crisp rule outputs, which is computationally less expensive then calculating the center of gravity.

The structure of TFC is shown in Figure 1, where *n* and *M* are, respectively, the number of input dimensions and the number of rules. It is a five-layer network structure. The functions of the nodes in each layer are described as follows:

Layer1 (*Input Node*): No function is performed in this layer. The node only transmits input values to layer 2. That is

$$u_i^{(1)} = x_i \tag{2}$$

Layer2 (Membership Function Node): Nodes in this layer correspond to one linguistic label of the input variables in layer1; that is, the membership value specifying the degree to which an input value belongs to a fuzzy set is calculated in this layer. For an external input x_i, the following Gaussian membership function is used:

$$u_{ij}^{(2)} = \exp\left(-\frac{\left[u_i^{(1)} - m_{ij}\right]^2}{\sigma_{ij}^2}\right) \tag{3}$$

where m_{ij} and σ_{ij} are, respectively, the center and the width of the Gaussian membership function of the *j*th term of the *i*th input variable x_i.

Layer 3 (Rule Node): The output of each node in this layer is determined by the fuzzy AND operation. Here, the product operation is utilized to determine the firing strength of each rule. The function of each rule is

$$u_j^{(3)} = \prod_i u_{ij}^{(2)} \tag{4}$$

Layer 4 (Consequent Node): Nodes in this layer are called consequent nodes. The input to a node in layer 4 is the output delivered from layer 3, and the other inputs are the input variables from layer 1 as depicted in Figure 1. For this kind of node, we have

$$u_j^{(4)} = u_j^{(3)}(w_{0j} + \sum_{i=1}^{n} w_{ij}x_i) \tag{5}$$

Where the summation is over all the inputs and where w_{ij} are the corresponding parameters of the consequent part.

Layer 5 (Output Node): Each node in this layer corresponds to one output variable. The node integrates all the actions recommended by layers 3 and 4 and acts as a defuzzifier with

$$y = u^{(5)} = \frac{\sum_{j=1}^{M} u_j^{(4)}}{\sum_{j=1}^{M} u_j^{(3)}} = \frac{\sum_{j=1}^{M} u_j^{(3)}(w_{0j} + \sum_{i=1}^{M} w_{ij}x_i)}{\sum_{j=1}^{M_k} u_j^{(3)}}$$

(6)

Where M is the number of fuzzy rule.

ISSN: 2277-3754
International Journal of Engineering and Innovative Technology (IJEIT)
Volume 1, Issue 4, April 2012

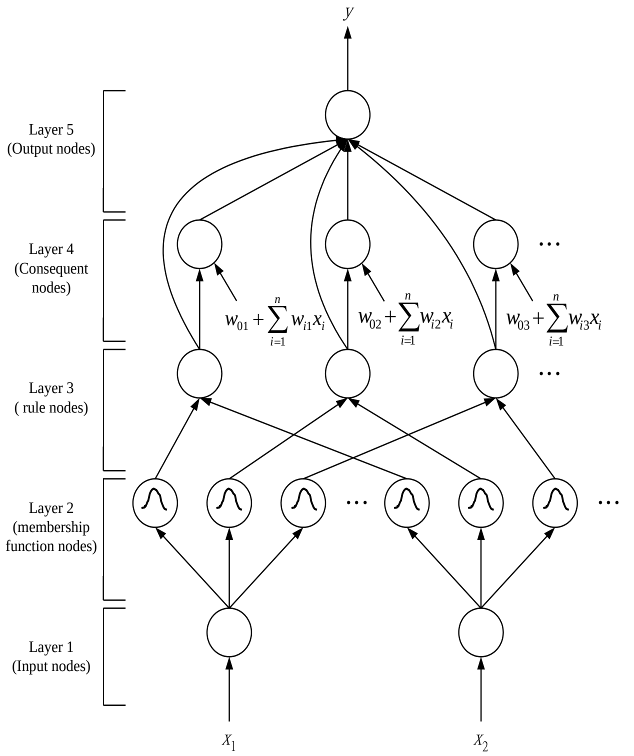

Fig. 1. The structure TSK-type fuzzy controller.

III. A MUTUALISM PARTICLE SWARM OPTIMIZATION (MPSO)

This section will introduce the proposed mutualism particle swarm optimization (MPSO) method. Recently, many researches try to enhance the traditional GAs have been made [34]-[37]. One category of them tries to modify the structure of a population. Examples in this category include the distributed GA [35], the cellular GA [36], and the symbiotic GA [37]. This study proposes the mutualism particle swarm optimization (MPSO) for improving the symbiotic GA [37]. In the proposed MPSO, the algorithm is developed from cooperative evolution. The idea of cooperative evolution was first proposed in an implicit fitness-sharing algorithm that is used in an immune system model [38]. The authors developed artificial antibodies to identify artificial antigens. Because each antibody can match only one antigen, a different population of antibodies is required to effectively defend against a variety of antigens. As shown in [13] and [37], partial solutions can be characterized as specializations. The specialization property ensures diversity, which prevents a population from converging to suboptimal solutions. A single partial solution cannot "take over" a population since there must exists other specializations. Unlike the standard evolutionary approach which always causes a given population to converge, hopefully at the global optimum, but often at a local one, the cooperative evolution find solutions in different, unconverted populations [13] and [37]. The MPSO is different from the traditional cooperative evolution; with each swarm in the MPSO is divided to several groups. Each group represents a set of the particles that belong to a fuzzy rule.

In the proposed MPSO, the structure of the swarm consists of several groups. Each group represents a set of the particles that belong to a fuzzy rule. The structure of the particle in the MPSO is shown in Figure 2. In the proposed MPSO, the coding structure of the particles must be suitable that each particle represent only one fuzzy rule. Figure 3 describes a fuzzy rule that had the form of Eq. (1) where m_{ij} and σ_{ij} represent a Gaussian membership function with mean and deviation with ith dimension and jth rule node.

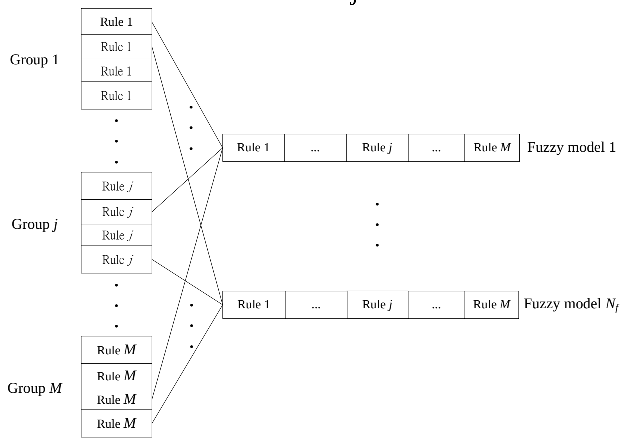

Fig.2. The structure of the particles in MPSO.

m_{1j}	σ_{1j}	m_{2j}	σ_{2j}	$\cdots$	m_{nj}	σ_{nj}	w_{0j}	w_{1j}	$\cdots$	w_{nj}

Fig. 3. Coding a rule of a TFC into a particle in the MPSO.

The learning process of the MPSO in each group involves three major operators: create initial swarms, evaluate fitness value and update each particle. The whole learning process is described step-by-step as follows:

A. Create Initial Swarms

Before the MPSO method is applied, every position $x_{j,k}$ must be created randomly in the range [0, 1] in each swarm, where j=1, 2… R represents the jth swarm and k=1, 2… ps represents the kth particle.

B. Evaluate Fitness Value

This subsection presents a novel method of cooperative evolution. As described above, in the cooperative evolution, the fitness value of a rule (a particle) is computed as the sum of the fitness values of all the feasible combinations of that rule with all other randomly selected rules, and then dividing this sum by the total number of combinations. Figure 2 shows the structure of the particle in the cooperative evolution. The stepwise assignment of the fitness value is as follows:

Step 0: Divide the rules into swarms of size *ps*.

Step 1: Randomly select *R* fuzzy rules (particles) from each of the above swarms, and compose the fuzzy system using these *R* rules.

Step 2: Calculate fitness value of the composed fuzzy system. In this study, the fitness value is given by the follow formula;

$$Fitness\ value=\frac{1}{1+\sqrt{\frac{1}{D}\sum_{d=1}^{D}\left(y_d-\bar{y}_d\right)^2}} \tag{7}$$

ISSN: 2277-3754
International Journal of Engineering and Innovative Technology (IJEIT)
Volume 1, Issue 4, April 2012

Where y_d represents the dth model output; $\bar{y}_d$ represents the desired output, and D represents the number of input data.

Step 3: Divide the fitness value by R and accumulate the divided fitness value to the fitness record of the R selected rules with their recorded fitness values initially set to zero.

Step 4: Repeat the above steps until each rule (particle) in each swarm has been selected a sufficient number of times, and record the number of fuzzy systems to which each particle has contributed.

Step 5: Divide the accumulated fitness of each particle by the number of times it has been selected.

C. Update Each Particle

Step 1: Update local best Lj,k and global best Gj

The local best position Lj,k is the best previous position that yielded the best fitness value of the jth swarm of the kth particle, and the global best position Gj is generated by the whole local best position. In step 1, the first step updates the local best position. Compare the fitness value of each current particle with that of its local best position. If the fitness value of the current particle exceeds those of its local best position, then the local best position is replaced with the position of the current particle. The second step updates the global best position. Compare the fitness value of all particles in their local best positions with that of the particle in the global best position. If fitness value of the particle in the local best position is better than those of the particles in the global best position, then the global best position is replaced with the current local best position.

$$L_{j,k} = \begin{cases} x_{j,k}, & \text{if } F(x_{j,k}) < F(L_{j,k}) \\ L_{j,k}, & \text{if } F(x_{j,k}) \geq F(L_{j,k}) \end{cases} \quad (8)$$
$$G_j = \arg\max_{L_{j,k}} F(L_{j,k}), \qquad 1 \leq k \leq ps$$

Step 2: Generate new swarms using $L_{j,k}$ and G_j

The step updates velocity and position of each particle to generate the new swarms using Eqs. (9) and (10).

$$v_{j,k}(t+1) = \omega \cdot v_{j,k}(t) + \phi_1 \cdot Rand() \cdot (L_{j,k} - x_{j,k}) + \phi_2 \cdot Rand() \cdot (G_j - x_{j,k}) \quad (9)$$
$$x_{j,k}(t+1) = x_{j,k}(t) + v_{j,k}(t+1) \quad (10)$$

Where ω is the coefficient of inertia, ϕ_1 is the cognitive study, ϕ_2 is the society study, and $Rand()$ is generated from a uniform distribution in the range [0, 1].

IV. LARYNGOPHARYNGEAL REFLUX DIAGNOSIS SYSTEM

A. Laryngeal structure feature extraction

Clinically, physicians use a flexible laryngoscope to capture the patient's laryngeal image. The condition can be diagnosed using its feature symptoms. First, a human laryngeal structure is divided into several parts, as shown in Figure 4. These include: (1) the arytenoids, A; (2) the interarytenoid area, B; (3) the vocal cords, C; (4) the epiglottis, E; (5) the false vocal cords, F; and (6) the subglottic area, G.

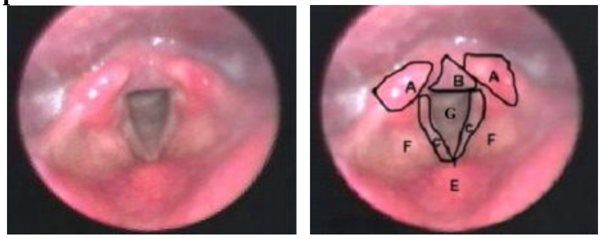

Fig. 4 Structural Drawing of Human Larynx.

The principal image and background image can be separated by processing with a combination of grey-level binary thresholding and filter. This binary image, *Im*, can be computed from following equation:

$$Im(u,v) = \begin{cases} 1 & ; \quad G(u,v) > Threshold \\ 0 & ; \quad otherwise \end{cases} \quad (11)$$

Experimental results show that the empirical value for the selection of threshold is 30. In processing continuous images, there will be a fixed ratio relationship in brightness between the selected feature and the whole image even though their brightness may be very different. Thus the selection of the threshold (T_2) should be appropriately adjusted in accordance with the average brightness (A_2) of every image. The results demonstrate that the variations in threshold in continuous images display a linear relationship at a fixed ratio. The feature area can be successfully separated using this relationship. The equation is as follows:

$$T_2 = T_1 + (A_2 - A_1) \quad (12)$$

Where A_1 the input is average brightness of the image and T_1 is the input threshold. The input threshold is determined using an empirical value which has been obtained from experimental results. When the average brightness of an image is between 98 and 100, the features of the subglottic area can be separated by a threshold of 60.

B. Segmentation of images

1. Segmentation of the arytenoids and the interarytenoid area

Segment the laryngeal image in Figure 5(a) using a deformable template et al [12]. The image can be transformed into grey-level first. This paper enhances the edge with G_x the weight of the gradient operator. The equation for the gradient operator is as follows:

The definition for image $f(x,y)$ in position (x,y) is as in equation (13) below:

$$\nabla f = \begin{bmatrix} G_x \\ G_y \end{bmatrix} = \begin{bmatrix} \frac{\partial f}{\partial x} \\ \frac{\partial f}{\partial y} \end{bmatrix} \quad (13)$$

Where G_x the gradient is weight on the x axis and G_y is the gradient weight on the y axis.

ISSN: 2277-3754
International Journal of Engineering and Innovative Technology (IJEIT)
Volume 1, Issue 4, April 2012

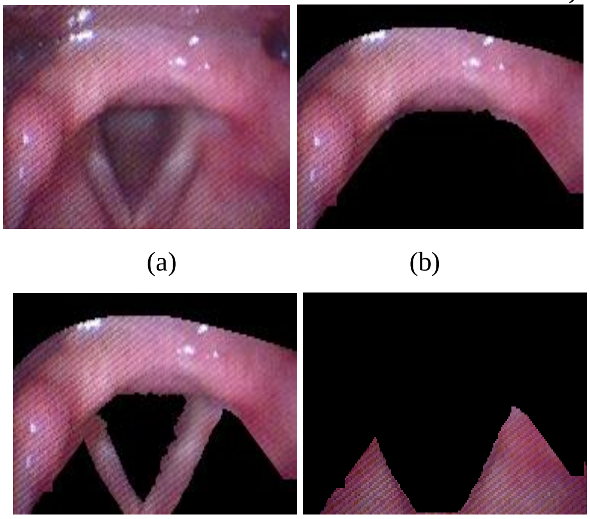

(a) (b)

(c) (d)

Fig 5 Experimental results of the boundary curve on the arytenoids and the interarytenoid area. (a)Original image; (b) Simulated boundary curve; (c) Results for segmentation of the arytenoids and vocal cords; (d) Results for segmentation of the false vocal cords.

The magnitude of this vector is a very important quantity in examining the edge, as shown in equation (14):

$$mag(\nabla f) = [G_x^2 + G_y^2]^{1/2} \qquad (14)$$

In addition, the direction of gradient weight is also a very important quantity. Given that $\alpha(x, y)$ represents the direction-angle of vector ∇f at (x, y), as shown in the equation (15):

$$\alpha(x, y) = \tan^{-1}\left(\frac{G_y}{G_x}\right) \qquad (15)$$

The angle is measured against the x axis. The direction at the edge of (x, y) is vertical against the direction of the gradient vector at this point.

Once the edge enhancement is completed, the edge of the arytenoids becomes obvious. Then the edge shape of the arytenoids can be described using a deformable template. The equation for the deformable template $\vec{V}(x, y)$ is as shown in equation (16):

$$\begin{cases} \begin{bmatrix} x \\ y \end{bmatrix} = \begin{bmatrix} t \\ -|t^{k_1}| \end{bmatrix} + \begin{bmatrix} x_0 \\ y_0 \end{bmatrix}; & t = 0,\ 1,\ \cdots,\ L_1 \\ \begin{bmatrix} x \\ y \end{bmatrix} = \begin{bmatrix} t \\ -|t^{k2}| \end{bmatrix} + \begin{bmatrix} x_0 \\ y_0 \end{bmatrix}; & t = -1,\ -2,\ \cdots,\ -L_2 \end{cases} \qquad (16)$$

where x_0, y_0, k_1, and k_2 are the parameters, x_0, y_0, k_1, and k_2 can be viewed as vector $P = (x_0, y_0, k_1, k_2)$, so that this paper can use the condition where the energy equation (17) is at maximum value to look for the most applicable vector P. Equation (17) is described as follow:

$$\begin{cases} E_{up} = \dfrac{1}{L_1 + L_2 + 1} \displaystyle\sum_{t=-L_2}^{L_1} G_x(\vec{V}) \\ E_{down} = \dfrac{1}{L_1 + L_2 + 1} \displaystyle\sum_{t=-L_2}^{L_1} (-1) \times G_x(\vec{V}) \end{cases} \qquad (17)$$

When $G_x(\vec{V})$ yields pixels which collectively correspond to curve $\vec{V}$ after the edge step, curve $\vec{V}(P)$ can be found with E_{up} at a maximum value. Curve $\vec{V}(P)$ may be the upper edge curve of the arytenoids and the interarytenoid area. Similarly, it can be also used to find curve $\vec{V}(P)$ with E_{down} at maximum value, which may be the lower edge curve of the arytenoids and the interarytenoid area. The results of the simulation are shown in Figure 5(b).

2 Segmentation of the vocal cords and the false vocal cords

Transform the image into grey-level and apply G_y weight in its gradient operator to carry out the task of edge enhancement. The edge of the vocal cords in the image can be simulated by using deformable template following edge enhancement. The definition for template $\vec{V}(x, y)$ is as shown in equation (18):

$$\begin{bmatrix} x \\ y \end{bmatrix} = \begin{bmatrix} r \\ 1 \end{bmatrix} \times t + \begin{bmatrix} x_0 \\ y_0 \end{bmatrix}; \qquad t = 1,\ 2,\ \cdots,\ N \qquad (18)$$

Where x_0, y_0, and r are parameters, this paper use the condition where the energy equation (19) is at maximum value to look for the optimum edge shape,

$$\begin{cases} E_1 = \dfrac{1}{N+1} \displaystyle\sum_{t=0}^{N} G_y(\vec{V}) \\ E_2 = \dfrac{1}{N+1} \displaystyle\sum_{t=0}^{N} (-1) \times G_y(\vec{V}) \end{cases} \qquad (19)$$

Where $G_y(\vec{V})$ is the pixels collectively corresponding to curve $\vec{V}$ after the edge step, the parameters, K_1 and K_2, are found corresponding to curve $\vec{V}(K)$ which gives E_1 and E_2 maximum values under the condition that $r > 0.2$. In addition, the parameters K_3 and K_4, corresponding to curve $\vec{V}(K)$, give E_1 and E_2 have maximum values under the condition that $r < -0.2$. After four straight lines have been determined with the deformable template, the connectivity of every line in the left and right directions can be computed. This means that the image of the vocal cords can be segmented. A disc structure element with a radius of two pixels is used to close it and then do the opening operation so that this paper can obtain a complete binary threshold image of the vocal cords and restore it to the corresponding pixel values of the original image. The image areas shown in Figure 5(c) are the vocal cords plus the arytenoids area and the interarytenoid area.
After completing segmentation of the arytenoids and the vocal cords, the results of Figure 5(c) are analyzed using connectivity analysis to mark the false vocal cords out, as shown in Figure 5(d).

ISSN: 2277-3754
International Journal of Engineering and Innovative Technology (IJEIT)
Volume 1, Issue 4, April 2012

V. SIMULATION

Simulation is discussed in this section. The example was run to evaluate the LRAGD-DS. For the simulations, the initial parameters are given in Table 1. The initial parameters are determined by practical experimentation or trial-and-error tests [39].

Table 1 The initial parameters before training.

Method	Training Accuracy			Testing Accuracy			CPU Time (Seconds)
	Best	Worst	Mean	Best	Worst	Mean	
MPSO	**96%**	**94%**	**95%**	**95%**	**91%**	**93%**	**93.17**
HELA [17]	89%	83%	87%	85%	80%	83%	138.73
GSE [41]	82%	74%	80%	80%	71%	76%	155.36
ESP [40]	80%	71%	79%	78%	69%	74%	161.77
SE [13]	79%	70%	75%	74%	67%	71%	168.52
GA [10]	73%	68%	71%	70%	63%	68%	153.62

Table 2 Comparison of performance for different methods.

Parameters	Value	Parameters	Value	Parameters	Value
Group Size	10	*Time Value*	10100	$[m_{\min}, m_{\max}]$	[0, 2]
Crossover Rate	0.5	*Desired Times*	10000	$[w_{\min}, w_{\max}]$	[-20, 20]
Mutation Rate	0.3	$[\sigma_{\min}, \sigma_{\max}]$	[0, 2]		

In this example, the simulation of MPSO- LRAGD-DS is discussed. There are 46 samples used to train the TFC-MPSO and 140 samples used to test TFC-MPSO. The values are floating-point numbers assigned using the MPSO initially. The fitness function in this example is defined in Eq. (10) to train TFC. There are ten fuzzy rules used to construct TFC. The evolution learning processed for 500 generations and is repeated 50 times. For comparative analysis, this paper uses the accuracy of grading to evaluate the performance of the LRAGD-DS. After 50 runs, the final training and testing average accuracy of three grades approximates 92% and 90%.

In this example, the same as example 1, in order to demonstrate the effectiveness and efficiency of the proposed TFC-MPSO, the SE, GA, and ESP are applied to the same problem. There are ten rules to construct the TFC. The parameters set for three methods are as follows: 1) the numbers of fuzzy rules are all set for 6; 2) the swarm sizes of SE and GA are 100 and 50 respectively; 4) the swarm size of the SE and ESP are both set for 50; 3) the crossover rates of SE, ESP, and GA are 0.55, 0.34, and 0.6, respectively; 3) the mutation rate of SE, ESP, and GA are 0.08, 0.14, and 0.12,respectively. The evolution learning processes for 500 generations and is repeated 50 times. After 50 runs, the final training average accuracy of the SE [13], ESP [40], and GA [10] approximate75%, 79%, and 71% and the final testing average accuracy of the SE [13], ESP [40], and GA [10] approximate 71%, 74%, and 68%.Table 2 lists the training accuracy, testing accuracy and CPU times of proposed method and other methods ([10, 13, 17, 40, and 41]). This experiment uses a Pentium III chip with an 800MHz CPU, a 512MB memory, and the visual C++ 6.0 simulation software. A total of thirty runs were performed. Clearly, Tables 2 shows that the proposed method can obtain shorter CPU time and better accuracy than other methods. As show in this example, we can find the situation of LRAGD can be diagnosed by the proposed MPSO automatically. Moreover, the performance of the MPSO is better than other methods.

VI. CONCLUSION

TSK-type fuzzy controllers (TFC) with mutualism particle swarm optimization (MPSO) for constructing laryngopharyngeal reflux associated gastrointestinal diseases diagnosis system (LRAGD-DS) are proposed in this paper. The advantages of the proposed MPSO are summarized as follows: 1) the MPSO uses group-based swarm to evaluate the fuzzy rule locally; 2) the MPSO can diagnose the situation of the LRAGD automatically. Therefore, this paper shows that the proposed method performs better than other methods through computer simulations.

ACKNOWLEDGMENT

This work was supported partially by the National Science Council under grant NSC 99-2221-E-009-148.

ISSN: 2277-3754
International Journal of Engineering and Innovative Technology (IJEIT)
Volume 1, Issue 4, April 2012

REFERENCES

[1] G. G. Towell and J. W. Shavlik, “Extracting refined rules from knowledge-based neural networks,” Machine Learning, vol.13, pp.71-101, 1993.

[2] C. J. Lin and C. T. Lin, “An ART-based fuzzy adaptive learning control network,” IEEE Transactions on Fuzzy Systems, vol.5, no.4, pp.477-496, 1997.

[3] C. F. Juang and C. T. Lin, “An on-line self-constructing neural fuzzy inference network and its applications,” IEEE Transactions on Fuzzy Systems, vol.6, no.1, pp.12-31, 1998.

[4] C. J. Lin and C. C. Chin, “Prediction and identification using wavelet-based recurrent fuzzy neural networks,” IEEE Transactions on Systems, Man and Cybernetics - Part B, vol.34, no.5, pp. 2144-2154, 2004.

[5] K. S. Narendra and K. Parthasarathy, “Identification and control of dynamical systems using neural networks,” IEEE Transactions Neural Networks, vol.1, no.1, pp.4-27, 1990.

[6] D. E. Goldberg, Genetic Algorithms in Search Optimization and Machine Learning, Reading, MA: Addison-Wesley, 1989.

[7] J. K. Koza, Genetic Programming: On the Programming of Computers by Means of Natural Selection, Cambridge, MA: MIT Press, 1992.

[8] L. J. Fogel, “Evolutionary programming in perspective: The top-down view,” in Computational Intelligence: Imitating Life, 1994.

[9] I. Rechenberg, “Evolution strategy,” in Computational Intelligence: Imitating Life, J. M. Zurada, R. J. Marks II, and C. Goldberg, Eds. Piscataway, NJ: IEEE Press, 1994.

[10] C. L. Karr, “Design of an adaptive fuzzy logic controller using a genetic algorithm,” Proceedings the Fourth International Conference on Genetic Algorithms, pp.450–457, 1989.

[11] C. C. Wong, H. Y. Wang, S. A. Li, and C. T. Cheng, “Fuzzy controller designed by GA for two-wheeled mobile robots,” International Journal of Fuzzy Systems, vol.9, no.1, pp.22-30, 2007.

[12] C. C. Wong, H. Y. Wang, and S. A. Li, “PSO-based motion fuzzy controller design for mobile robots,” International Journal of Fuzzy Systems, vol.10, no.1, pp.284-292, 2008.

[13] C. F. Juang, J. Y. Lin and C. T. Lin, “Genetic reinforcement learning through symbiotic evolution for fuzzy controller design,” IEEE Transactions on Systems, Man and Cybernetics - Part B, vol.30, no.2, pp.290-302, 2000.

[14] K. S. Tang, Genetic algorithms in modeling and optimization, Ph.D. Dissertation, Dep. Electron. Eng., City Univ. Hong Kong, 1996.

[15] C. F. Juang, “Combination of online clustering and Q-value based GA for reinforcement fuzzy system design,” IEEE Transactions Fuzzy Systems, vol.13, no.3, pp.289–302, 2005.

[16] C. J. Lin and Y. J. Xu, “Efficient Reinforcement Learning through Dynamical Symbiotic Evolution for TSK-Type Fuzzy Controller Design,” International Journal of General Systems, vol.34, no.5, pp.559-578, 2005.

[17] C. J. Lin and Y. C. Hsu, “Reinforcement Hybrid Evolutionary Learning for Recurrent wavelet-based neuro-fuzzy controllers,” IEEE Transactions on Fuzzy Systems, vol.15, no.4, pp.729-745, 2007.

[18] F. A. Levente, A. Razvan, J. C. Catharine, A. W. Sarah and S. Nicholas, “A genetic algorithm optimized fuzzy neural network analysis of the affinity of inhibitors for HIV-1 protease,” Bioorganic & Medicinal Chemistry, vol.16, no.6, pp.2903-2911, 2008.

[19] N. Benamrane, A. Aribi, L. Kraoula, Fuzzy Neural Networks and Genetic Algorithms for Medical Images Interpretation, IEEE Proc. of the conf. on Geometric Modeling and Imaging: New Trends, 2006.

[20] S. Wang, D. Fu, M. Xu and D. Hu, “Advanced fuzzy cellular neural network: Application to CT liver images,” Artificial Intelligence in Medicine, vol.39, no.1, pp.65-77, 2007.

[21] S. Wang, F. L. C. Korris and D. Fu, “Applying the improved fuzzy cellular neural network IFCNN to white blood cell detection,” Neurocomputing, vol.70, no.7, pp.1348-1359, 2007.

[22] A. Subasi, “Automatic detection of epileptic seizure using dynamic fuzzy neural networks,” Expert Systems with Applications, vol.31, no.2, pp.320-328, 2006.

[23] D. T. Lin, C. R. Yan and W. T. Chen, “Autonomous detection of pulmonary nodules on CT images with a neural network-based fuzzy system,” Computerized Medical Imaging and Graphics, vol.29, no.6, pp.447-458, 2005.

[24] S. R. Chowdhury and H. Saha, “Development of a FPGA based fuzzy neural network system for early diagnosis of critical health condition of a patient,” Computers in Biology and Medicine, vol.40, no.2, pp.190-200, 2010.

[25] H. B. Ebadian, H. S. Zadeh, S. Setayeshi and S. T. Smith, “Neural network and fuzzy clustering approach for automatic diagnosis of coronary artery disease in nuclear medicine,” IEEE Transactions on Nuclear Science, vol.51, no.1, pp.1 84-192, 2004.

[26] P. C. Belafsky, G. N. Postma, and J.A. Koufman, “The validity and reliability of the reflux finding score (RFS)”, Laryngoscope, vol.111, no.8, pp.1313-1317, 2001.

[27] R. K. Hill, C. B. Simpson, R. Velazquez, and N. Larson, “Pachydermia is not diagnostic of active laryngopharyngeal reflux disease,” Laryngoscope, vol.114, no.9, pp.1557-1561, 2004.

[28] M. E. Beaver, C. R. Stasney, E. Weitzel, M. G. Stewart, D. T. Donovan, and R. B. Parke, “Diagnosis of laryngopharyngeal reflux disease with digital imaging,” Otolaryngology-Head Neck Surgery, vol.128, no.1, pp.103-108, 2003.

[29] L. Arango, A. Angel, R. I. Molina, and J. R. Marquez, “Comparison between digestive endoscopy and 24-hour esophageal pH monitoring for the diagnosis of gastro esophageal reflux esophagitis：Presentation of 100 cases,” Hepato-Gastroenterology, vol.47, no.31, pp.174-180, 2000.

[30] D. G. Hanson, J. Jiang, and W. Chi, “Quantitative color analysis of laryngeal erythema in chronic posterior laryngitis,” Journal of Voice, vol.12, no.1, pp.78-83, 1998.

[31] J. F. R. Ilgner, C. Palm, A. G. Schutz, K. Spitzer, M. Westhofen, and T. M. Lehmann, “Colour texture analysis for quantitative laryngoscopy,” Acta Otolaryngol, vol.123, pp.730-734, 2003.

[32] S. Men, M. C. Ecevit, I. Topcu, N. Kabakci, T. K. Erdag, and S. Sutay, "Diagnostic Contribution of Virtual Endoscopy in Diseases of the Upper Airways," Journal of Digital Imaging, vol.20, no.1, pp.67-71, 2007.

[33] T. Takagi and M. Sugeno, "Fuzzy identification of systems and its applications to modeling and control," IEEE Transactions on Systems, Man and Cybernetics, vol.15, no.1, pp.116-132, 1985.

[34] Z. Michalewicz, Genetic Algorithms+Data Structures=Evolution Programs. New York: Springer-Verlag, 1999.

[35] R. Tanese, "Distributed genetic algorithm," Proc. Int. Conf. Genetic Algorithms, pp. 434–439, 1989.

[36] J. Arabas, Z. Michalewicz, and J. Mulawka, "GAVaPS—A genetic algorithm with varying population size," Proceedings IEEE Int. Conference Evolutionary Computation, Orlando, pp. 73–78, 1994.

[37] D. E. Moriarty and R. Miikkulainen, "Efficient reinforcement learning through symbiotic evolution," Machine Learning, vol.22, no.1, pp.11–32, 1996.

[38] R. E. Smith, S. Forrest, and A. S. Perelson, "Searching for diverse, cooperative populations with genetic algorithms," Evolutionary Computation, vol.1, no.2, pp.127–149, 1993.

[39] J. J. Grefenstette, "Optimization of control parameters for genetic algorithms," IEEE Transactions on Systems, Man and Cybernetics, vol.6, no.1. pp. 122–128, 1986.

[40] F. J. Gomez, Robust non-linear control through neuroevolution, Ph.D. Disseration, The University of Texas at Austin, 2003.

[41] C. J. Lin and Y. J. Xu, "A Self-Adaptive Neural Fuzzy Network with Group-Based Symbiotic Evolution and Its Prediction Applications," Fuzzy Sets and Systems, vol.157, no.8, pp.1036-1056, 2006.

AUTHORS PROFILE

Cheng-Hung Chen was born in Kaohsiung, Taiwan, R.O.C. in 1979. He received the B.S. and M.S. degree in Computer Science and Information Engineering from the Chao-yang University of Technology, Taiwan, R.O.C., in 2002 and 2004. He is currently working toward the Ph.D. degree in Electrical and Control Engineering at National Chiao Tung University, Taiwan, R.O.C. His current research interests are neural networks, fuzzy systems, evolutionary algorithms, intelligent control, and pattern recognition.

Hsien-Tse Chen was born in Taipei, Taiwan, R.O.C., in 1977. He received the B.S. degree in department of marine engineering from National Taiwan Ocean University, Keelung, Taiwan, R.O.C, in 1999 and the M.S. degree in department of automatic control engineering from Feng Chia University, Taichung, Taiwan, R.O.C, in 2002. He is currently pursuing the Ph. D. degree in the Department of Electrical and Control Engineering, the National Chiao Tung University, Hsinchu, Taiwan. His current research interests include image recognition, medicine image processing, machine vision.

Sheng-Fuu Lin (S'84–M'88) was born in Taiwan, R.O.C., in 1954. He received the B.S. and M.S. degrees in mathematics from National Taiwan Normal University in 1976 and 1979, respectively, the M.S. degree in computer science from the University of Maryland, College Park, in 1985, and the Ph.D. degree in electrical engineering from the University of Illinois, Champaign, in 1988. Since 1988, he has been on the faculty of the Department of Electrical and Control Engineering at National Chiao Tung University, Hsinchu, Taiwan, where he is currently a Professor. His research interests include image processing, image recognition, fuzzy theory, automatic target recognition, and scheduling